19

Research paper
Doi 10.61892/STP202601058M
ISSN 2566-4484

STEPGRAD
СТЕПГРАД

Vuk Milošević, University of Nis, vukamer@gmail.com
Dragan Kostić, University of Nis, dragan.kostic@gaf.ni.ac.rs
Snežana Đorić Veljković, University of Nis, snezana.djoric.veljkovic@gaf.ni.ac.rs
Sonja Krasić, University of Nis, sonja.krasic@gaf.ni.ac.rs

THERMAL MEASUREMENTS ON A MEMBRANE-COVERED SPORTS FACILITY: CASE STUDY IN NIŠ, SERBIA

Abstract:

There are numerous membrane-covered sports facilities in Niš. They have become popular over the last two decades due to their low cost and rapid construction. However, they are known to provide poor indoor thermal conditions, and methods for improving their performance are still being investigated. This research forms part of that effort. A typical membrane-covered facility, the physical education hall of Ivan Goran Kovačić School in Niš, was selected for analysis. Several thermal parameters were measured during a hot summer day. The results confirmed some findings reported in previous research, but also contradicted certain expectations. The conclusions of this study will be used to propose improved thermal solutions for membrane-covered sports facilities.

Keywords: membrane structures, sports facilities, thermal properties.

МЕРЕЊА ТЕРМИЧКИХ ПАРАМЕТАРА НА СПОРТСКОЈ БАЛОН ХАЛИ: СТУДИЈА СЛУЧАЈА У НИШУ, СРБИЈА

Сажетак:

У Нишу постоји већи број спортских балон хала. Оне су постале популарне у последње две деценије, пре свега због мале цене коштања и кратког времена изградње, у поређењу са другим типовима конструкција. Познате су и по лошим термичким карактеристикама, на чијем се унапређењу и даље ради. Ово истраживање је део таквих тежњи. Типична спортска балон хала у Нишу је изабрана за анализу. Више термичких параметара праћено је током топлог летњег дана. Резултати су потврдили одређене закључке претходних истраживања, али су и пркосили неким од постављених очекивања. Закључци овог истраживања биће коришћени приликом предлагања унапређеног решења спортске балон хале.

Кључне речи: мембранске конструкције, спортски објекти, термика.

1. INTRODUCTION

In the search for cost-effective design solutions for sports facilities, membrane-covered buildings have emerged as a viable option. Low construction costs combined with short construction times provide an affordable way to enclose sports fields and protect them from rain and snow. However, reduced initial investment often results in compromised indoor thermal comfort and increased operational energy demand. The primary cause is the extreme thinness of the membrane material, which results in very low thermal resistance.

In certain climates, this limitation may be less critical. In Serbia and the Western Balkans region, a significant number of membrane-covered sports facilities have been constructed over the past two decades. This might suggest that the regional climate is suitable for such structures. However, users frequently report dissatisfaction with indoor thermal comfort levels. Therefore, a broader study aimed at measuring thermal conditions inside membrane-covered sports facilities has been initiated. This paper presents results from one summer day of measurements conducted at a sports facility in Niš, Serbia.

Previous research has investigated thermal comfort of similar small sports facilities [1]. Basic measurements were conducted on a facility in Montenegro [2]. Comparisons between single and double-layer membrane systems have also been reported [3]. Different types of air-supported membrane-covered sports facilities were examined [4]. Several other studies on membrane-covered air-supported stadiums exist [5], [6], [7]. Although these structures are primarily used to cover sports fields and arenas, they are also applied in industrial buildings [8], where indoor thermal requirements may differ significantly depending on function. A review of studies on the thermal environment in buildings covered by membranes is has been done [9]. Indoor thermal comfort of membrane covered facilities is analyzed [10], [11], [12]. Numerical modeling can be used to evaluate alternative design solutions and optimize thermal performance [13]. However, a comprehensive life-cycle cost and energy analysis of a typical membrane-covered sports facility has yet to be conducted.

2. METHODOLOGY

The research presented in this paper analyzes a single membrane-covered sports facility located in Niš, Serbia. Its location is shown in Figure 1. The building serves as a physical education hall for Ivan Goran Kovačić Primary School, situated in the Nikola Tesla suburb. The longitudinal axis of the building is oriented in the north–south direction. The facility measures approximately 18x31 m and is fully enclosed with a membrane envelope. Parts of longitudinal membrane walls can be opened during summer for ventilation. On the west side, it is connected to the main school building by an annex containing toilets and changing rooms. The facility is fenced on all other sides. The surrounding area is shown in Figure 2.

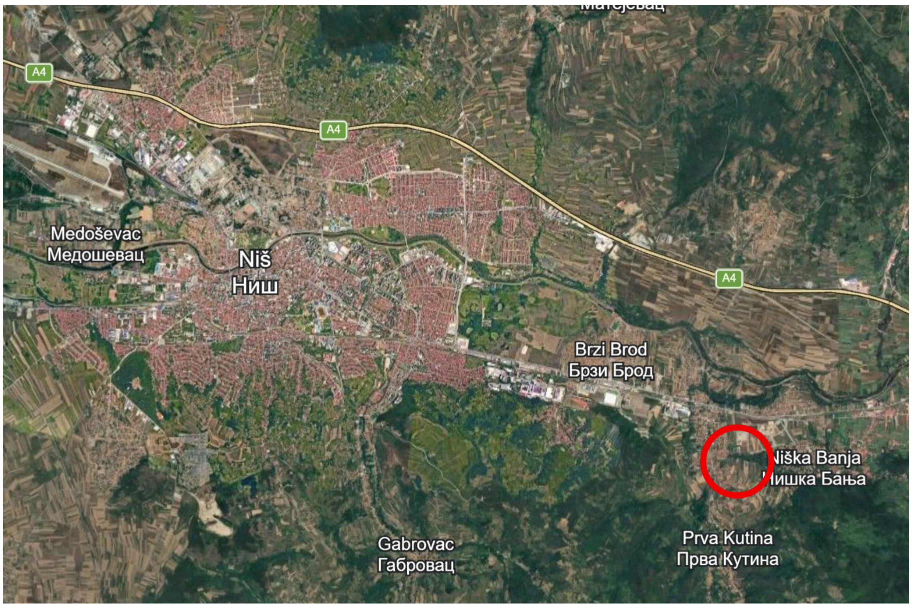

Figure 1. Location of the analyzed sports facility (source: Google Earth).

Figure 2. Near-by surroundings of the analyzed sports facility (source: Google Earth).

The supporting structure is made of steel. The main steel arches are trussed with diagonal and vertical web members. The arch geometry is polygonal. Five rows of purlins are installed; all are straight, and the top row is trussed. The end walls are supported by a combination of steel columns, including one trussed steel column, and steel beams. The enclosure membrane is of the PVC/PES type. The end walls and lower roof sections are green, while the remaining roof area is white. Exterior and interior views of the facility are shown in Figures 3 and 4.

Figure 3. Exterior view of the analyzed sports facility (source: photograph by authors).

Figure 4. Interior view of the analyzed sports facility (source: photograph by authors).

Measurements were conducted on 26 July 2025, during a hot summer day. The available equipment included one Sygonix SY-5479628 meteorological station, four Testo Saveris 2-T2 data loggers each coupled with a surface temperature probe, three Testo Saveris 2-H1 integrated temperature sensors, and two Testo 160 THL integrated temperature and humidity sensors.

The sensors were mounted on a central supporting arch, as shown in Figure 5. The arch was divided into six segments, and sensors were installed at the upper five vertices. These measurement points were labeled 1 to 5, from east to west. Points 1 and 5 are located at the same height; points 2 and 4 are positioned above them; and point 3 is located at the apex of the arch. The meteorological station was placed inside the building, in the northwest corner (Figure 5), due to the requirement for a constant power supply. Its external unit was installed nearby, above the annex (Figure 6).

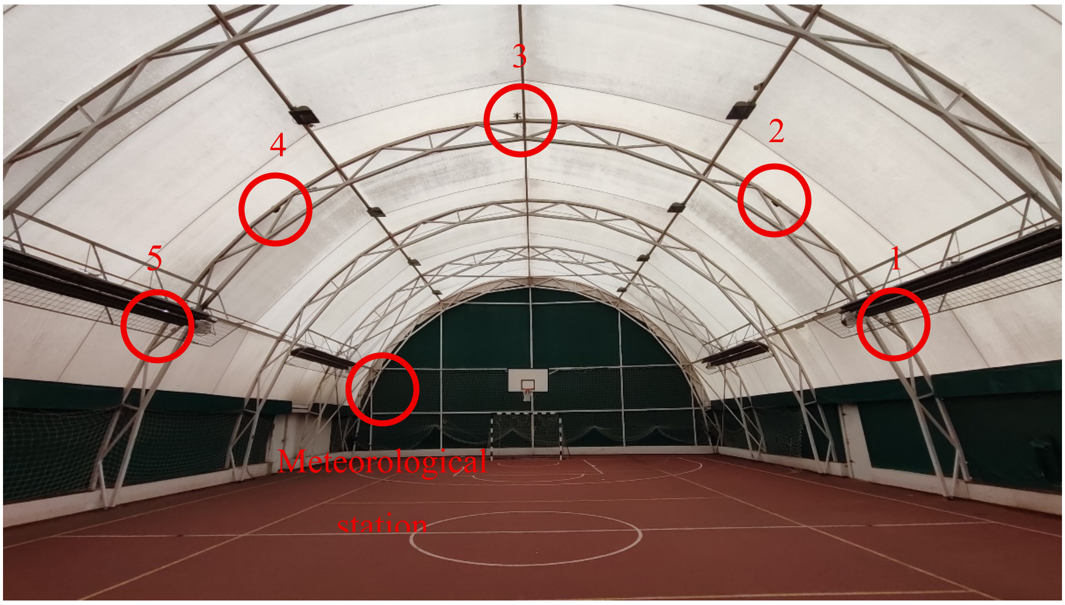

Figure 5. Set-up of the measuring devices inside the facility (source: photograph by authors).

Figure 6. Internal and external part of the meteorological station (source: photographs by authors).

The measurement setup was designed to capture several key parameters. The meteorological station records indoor and outdoor air temperatures, enabling direct comparison. It also measures solar irradiance, which is critical for understanding the thermal behavior of the membrane cover. Additionally, air pressure, precipitation, and wind speed were recorded, as these factors may influence indoor thermal comfort.

The distributed sensors were intended to provide two primary datasets. First, air temperature measurements at different heights allow evaluation of vertical thermal stratification within the facility. Second, surface temperature probes measure the membrane surface temperature to assess the impact of solar radiation. Due to the building's orientation and sensor placement, the results are expected to reveal the sensitivity of the membrane to varying angles of solar incidence.

3. RESULTS

The equipment was configured to automatically record all measured values and store them in the cloud. The recording interval was set to 15 minutes for both the meteorological station and the sensors. Data were monitored during the measurement period and downloaded after the selected measurement day. The date 26 July 2025 was chosen as one of the hottest days of the year. The results are presented in graphical form in the following subsections.

3.1. METEOROLOGICAL STATION RECORDINGS

The meteorological station recorded several parameters. Air temperature measurements are shown in Figure 7. Two datasets are presented: outdoor air temperature and indoor air temperature at the location of the station. The values are plotted for the entire day at 15-minute intervals. Recorded values of solar irradiance and air pressure are presented together in Figure 8. The irradiance scale is shown on the left axis of the chart, while air pressure is shown on the right axis. The official astronomical sunrise time was 05:17, and sunset occurred at 19:59. Although the equipment allows measurement of precipitation, rainfall during the measurement day was negligible. A total of 0.3 mm was recorded at 21:45, reaching a cumulative 0.5 mm at 22:00. Due to the minimal amount, precipitation data are not plotted. Wind data are presented in Figure 9, which shows both wind speed and wind gust values. Wind direction was also recorded but is not included in the charts.

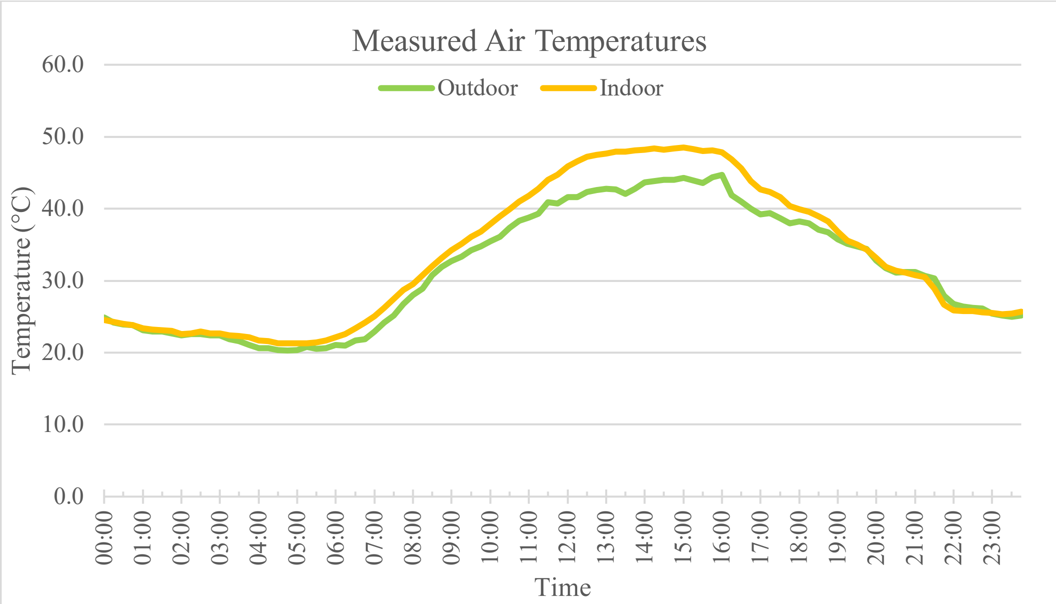

Figure 7. Measured air temperatures (source: diagram by authors)

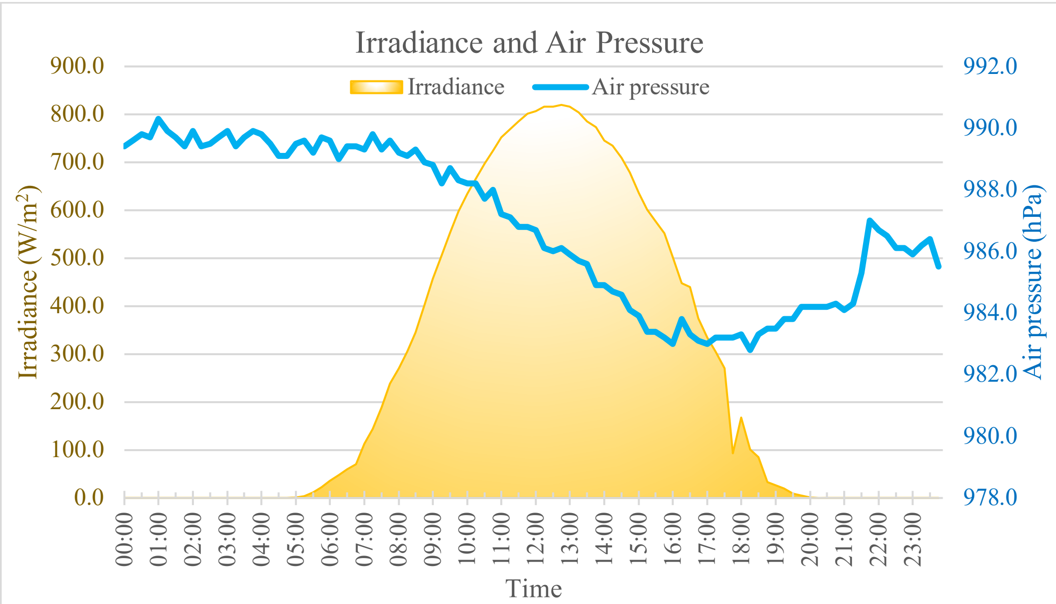

Figure 8. Measured irradiance and air pressure (source: diagram by authors)

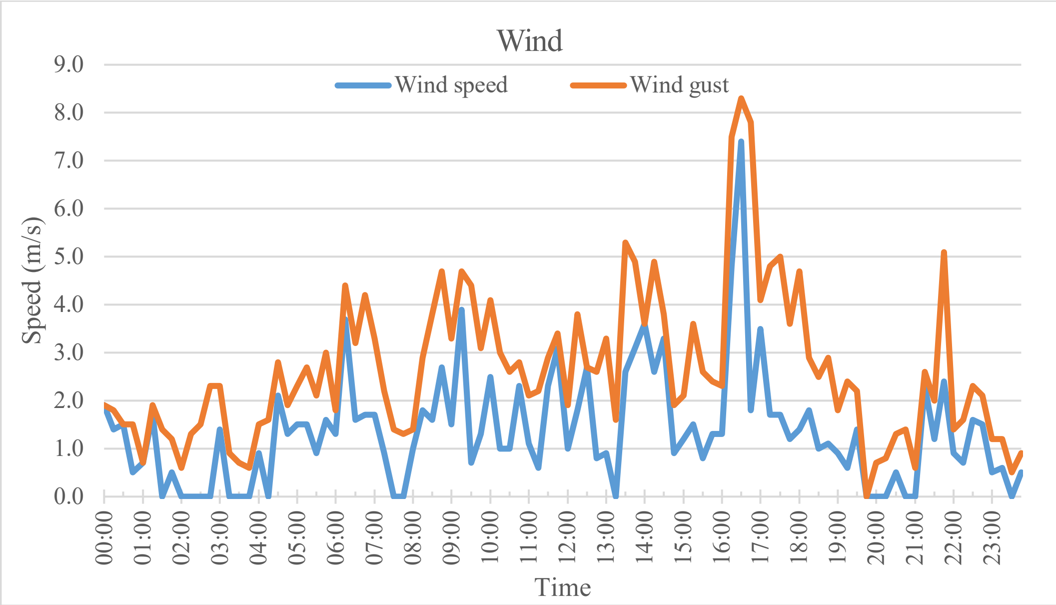

Figure 9. Measured wind parameters (source: diagram by authors)

3.2. SENSOR RECORDINGS

Sensors were labeled according to their position and the type of data recorded. The first part of each label denotes the measurement point, while "AT" refers to air temperature and "ST" to surface temperature. Five sensors measured indoor air temperature, one at each point. Their results are presented in Figure 10. It was initially expected that point 3 (the highest point of the arch) would consistently record the highest temperature due to thermal stratification. Conversely, points 1 and 5 (the lowest positions) were expected to continually record the lowest air temperatures.

Surface temperatures of the membrane are shown in Figure 11. Although the membrane is white, it is known to heat significantly under solar radiation. Due to the arched geometry of the roof, different sections are exposed to solar radiation at varying incident angles throughout the day. Surface sensors were placed at four points to capture this effect. The fifth point was not instrumented for surface temperature due to the limited number of available probes.

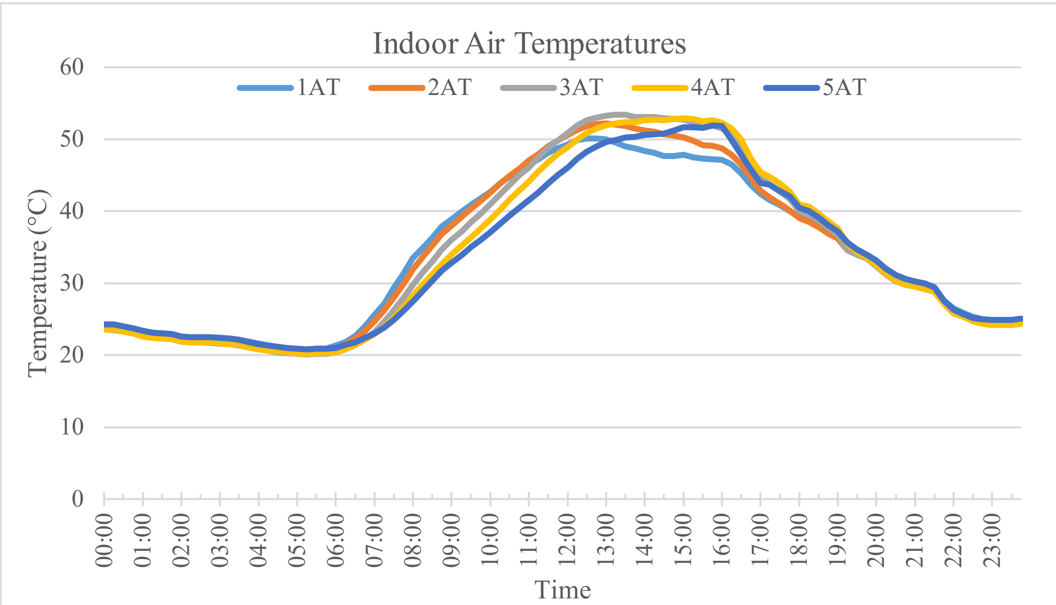

Figure 10. Measured indoor air temperatures (source: diagram by authors)

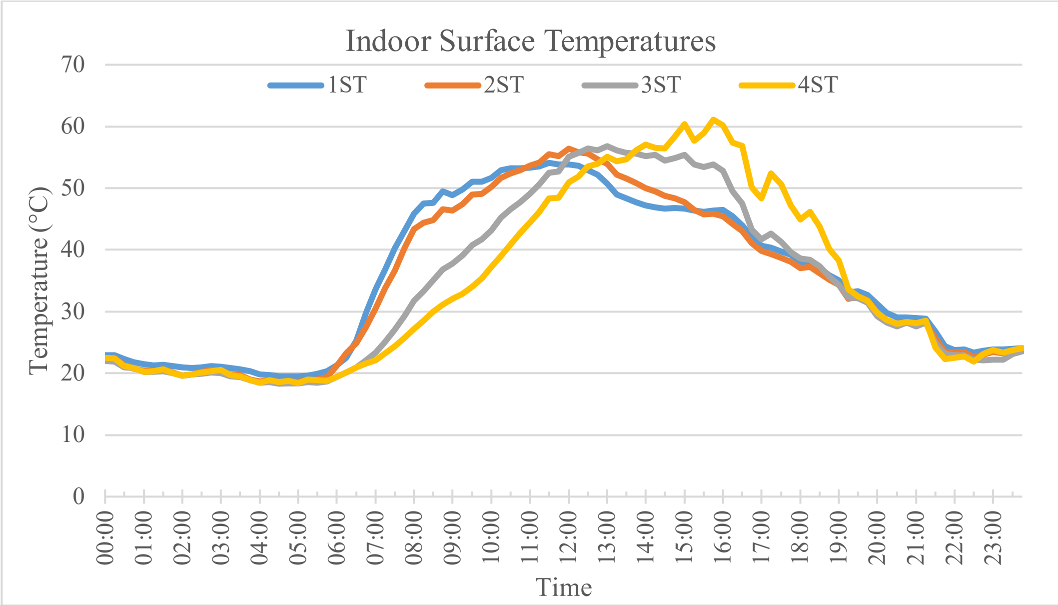

Figure 11. Measured indoor surface temperatures (source: diagram by authors)

4. DISCUSSION

The recorded data revealed several interesting behaviors, some of which contradicted expectations while others confirmed findings from previous research. Figure 7 presents the outdoor and indoor air temperatures. From midnight to 03:00, the two temperatures were nearly identical. Both continued to decrease until 04:45, with the outdoor temperature dropping approximately 1°C lower than the indoor temperature. Both temperatures began to rise at 05:30.

The indoor temperature increased steadily until 12:30 at a rate of approximately 3.7°C per hour. It then plateaued at around 48°C until 16:00, reaching a maximum of 48.5°C. The outdoor temperature increased at 3.9°C/h until 08:30, then at 3°C/h until 11:30, and finally at 1°C/h until 16:00, when it reached a maximum of 44.7°C. After 16:00, both temperatures declined and converged at approximately 19:45. Throughout the day, the indoor temperature remained higher than the outdoor temperature, with the largest difference (5.8°C) recorded at 13:30.

This behavior was expected, as membrane structures lack significant thermal mass and insulation compared to conventional building materials, which typically provide thermal lag and buffering effects. The limited thermal resistance of thin membranes restricts their broader application in hot climates.

Figure 8 shows air pressure and solar irradiance. Air pressure generally varied inversely with outdoor temperature, ranging between 982 and 991 hPa. Solar irradiance began increasing at 05:00 and reached a peak of 819.9 W/m² at 12:45. It then gradually declined, except for a noticeable drop at 17:45, likely caused by cloud cover. After 20:30, there was no recorded irradiance.

Wind data (Figure 9) indicate that wind speeds remained below 4 m/s for most of the day, with gusts generally below 5.5 m/s. According to the Beaufort scale, wind speeds between 3.4 and 5.5 m/s correspond to a gentle breeze. Only around 16:30 did wind speed and gust reach 7.4 m/s and 8.3 m/s, corresponding to moderate to fresh breeze conditions. Overall, wind influence on indoor temperatures was minimal.

The indoor air temperatures are analyzed next and are shown in Figure 10. During the early part of the day, the temperatures are nearly identical, differing by less than 1°C until 6:00. They decrease steadily until 5:15, after which they begin to rise. Initially, the air temperature at point 1 becomes the highest, followed by point 2, while lower temperatures are recorded at points 3, 4, and 5, respectively. This behavior was not anticipated, as it was expected that the highest point of the arch (point 3) would consistently record the highest temperature due to thermal stratification. At 10:30, point 2 records the highest temperature. By 12:00, point 3 becomes the warmest location. At 15:00, point 4 shows the highest temperature, and finally, at 19:15, point 5 records the highest air temperature.

The maximum temperature at point 1 reaches 50.1°C at 12:30. At point 2, the maximum recorded temperature is 52.2°C at 13:00. Point 3, the highest point of the arch, records the overall maximum air temperature of 53.4°C at 13:30. The temperature at point 4 rises to 52.9°C at 15:00, while the highest recorded temperature at point 5 is 51.9°C at 15:45. To explain why these temperatures did not follow the initially expected stratification pattern, it is necessary to examine the surface temperature results. A comparison between air temperatures recorded by the distributed sensors and those recorded by the meteorological station shows that the sensor values are consistently higher. This difference can be attributed to the position of the meteorological station near the north wall, which remains shaded and is located at a lower height than the arch-mounted sensors, resulting in lower recorded air temperatures.

Membrane surface temperatures at different points are presented in Figure 11. The values remain very close until 5:30, when the surface at point 1 begins to warm up rapidly. It is followed closely by point 2, while the surfaces at points 3 and 4 warm up more gradually. At 11:00, point 2 records the highest surface temperature. At 12:30, point 3 becomes the hottest, and by 13:45, point 4 records the highest surface temperature. The maximum surface temperature at point 1 is 54.1°C at 11:30. At point 2, the maximum recorded surface temperature is 56.4°C at 12:00. Point 3 reaches 56.8°C at 13:00, while point 4 records the highest overall surface temperature of 61.1°C at 15:45.

Since point 1 is oriented eastward, it receives direct sunlight first in the morning, with a smaller incident angle compared to the other points, while points 4 and 5 remain in shade. As the sun rises and moves westward, the incident angles at the remaining points decrease sequentially, causing the highest surface temperatures to shift gradually from east to west. When comparing the air temperature results with the surface temperature data, it becomes clear why the expectation that point 3 would consistently record the highest air temperature was not met. Although thermal stratification is present, indoor air temperatures are strongly influenced by the temperature of the adjacent membrane surface. The highest air temperatures at each measurement point closely follow the peak surface temperatures of the corresponding membrane sections. This finding further confirms conclusions from previous research indicating that membrane temperature is primarily governed by outdoor air temperature and solar irradiance, while indoor air temperature is significantly influenced by membrane surface temperature.

5. CONCLUSIONS

This study presents thermal measurements of a typical membrane-covered sports facility located adjacent to Ivan Goran Kovačić Primary School in Niš. Measurements were conducted on 26 July 2025, one of the hottest days of the year. Recorded parameters included solar irradiance, wind speed, precipitation, outdoor air temperature, indoor air temperature at multiple heights, and membrane surface temperature at multiple roof locations. Sensor placement was designed to capture spatial variations along the roof cross-section. The objective was to collect data that could inform the development of improved membrane-covered facilities with enhanced thermal performance.

The results revealed several important patterns. Indoor air temperature significantly exceeded outdoor air temperature during peak hours. Membrane surface temperatures reached even higher values, as expected under strong solar radiation. However, it was not anticipated that the highest indoor air temperatures would shift sequentially from east to west across the roof cross-section, following solar exposure. This behavior demonstrates the strong influence of membrane surface temperature on indoor thermal conditions. During hot summer days, this effect is unfavorable and needs to be mitigated to improve user comfort in membrane-covered sports facilities.

ACKNOWLEDGEMENT

This research was supported by the Science Fund of the Republic of Serbia, Grant No. 7363, Improvement of functional, energetic, lightening and structural characteristics of closed and semi closed halls covered by structural textile membranes - BALLOON-HALL-Optima.

LITERATURE

[1] A. Silvestri, N. Paraciani, and T. Villani, “Performance evaluation of textile materials for lightweight envelopes in minor sports facilities and their impact on indoor comfort,” *Archit. Eng. Des. Manag.*, vol. 17, no. 3–4, pp. 347–359, 2021.

[2] V. Milošević, M. Jevrić, O. Ćalasan, and N. Ranđelović, “The relation between indoor and outdoor air temperatures in membrane-covered building,” in *Proc. VI Energy Efficiency Symp.*, Banja Luka, Bosnia and Herzegovina, Jun. 12–13, 2025.

[3] D. Kostić, V. Milošević, V. Bogdanović, M. Vasov, and A. Vučur, “Influence of single and double membrane roofs on thermal behaviour of enclosed space,” *Teh. Vjesn.*, vol. 25, suppl. 1, pp. 188–196, 2018, doi: 10.17559/TV-20161205160405.

[4] A. Alongi, A. Angelotti, A. Rizzo, and A. Zanelli, “Measuring the thermal resistance of double and triple layer pneumatic cushions for textile architectures,” *Archit. Eng. Des. Manag.*, vol. 17, no. 3–4, pp. 334–346, 2021, doi: 10.1080/17452007.2020.1740152.

[5] H. Suo, A. Angelotti, and A. Zanelli, “Thermal-physical behavior and energy performance of air-supported membranes for sports halls,” *Energy Build.*, vol. 109, pp. 35–46, 2015, doi: 10.1016/j.enbuild.2015.10.011.

[6] I. Tariq, W. Chen, Y. Yue, and C. Gao, “Long-term thermal performance analysis of an air-supported membrane structure with advanced thermal insulation design,” *Energy Build.*, vol. 351, Art. no. 116743, 2026, doi: 10.1016/j.enbuild.2025.116743.

[7] C. Huang, Y. Sun, H. Wang, M. Pang, W. Wang, and W. Wei, “Thermal performance analysis and optimization of air-supported membrane building envelope based on numerical simulation,” *Thin-Walled Struct.*, vol. 206, Art. no. 112615, 2025, doi: 10.1016/j.tws.2024.112615.

[8] G. Tian, Y. Fan, H. Wang, K. Peng, X. Zhang, and H. Zheng, “Studies on the thermal environment and natural ventilation in industrial building spaces enclosed by fabric membranes,” *J. Build. Eng.*, vol. 32, Art. no. 101651, 2020, doi: 10.1016/j.jobe.2020.101651.

[9] G. J. Tian, Y. S. Fan, M. Gao, H. Wang, H. Zheng, J. Liu, and C. Liu, “Indoor thermal environment of thin membrane structure buildings: A review,” *Energy Build.*, vol. 234, Art. no. 110704, 2021, doi: 10.1016/j.enbuild.2020.110704.

[10] J. Hu, W. Chen, S. Zhang, Y. Yin, Y. Li, and D. Yang, “Thermal characteristics and comfort assessment of enclosed large-span membrane stadiums,” *Appl. Energy*, vol. 229, pp. 728–735, 2018, doi: 10.1016/j.apenergy.2018.08.033.

[11] Y. Bai, L. Zhao, R. Tang, and X. Kang, “Study on winter thermal comfort of membrane structure gymnasium in severe cold region of China,” *Sci. Technol. Built Environ.*, vol. 28, pp. 499–511, 2022, doi: 10.1080/23744731.2021.2018874.

[12] R. Li, Y. Liu, G. Yu, H. Guo, and S. Qin, “Establishment of a thermal comfort model for spectator areas of air-supported membrane ice rinks in severe cold regions,” *Energies*, vol. 16, Art. no. 4598, 2023, doi: 10.3390/en16124598.

[13] D. Ranđelović, M. Vasov, D. Kostić, V. Jovanović, J. Savić, and A. Anđelković, “Energy efficiency and indoor microclimate in balloon halls: A case study on thermal stability and ventilation simulation,” in *Proc. 10th Int. Conf. Smart Sustain. Technol. (SpliTech)*, Split–Bol, Croatia, Jun. 16–20, 2025.